J Math Chem (2009) 46:811–819
DOI 10.1007/s10910-009-9551-3

ORIGINAL PAPER

Two approaches for modelling hydrate growth

Trygve Buanes · Bjørn Kvamme · Atle Svandal

Received: 2 January 2007 / Accepted: 30 September 2008 / Published online: 25 July 2009
© Springer Science+Business Media, LLC 2009

Abstract We consider two different approaches to model growth of CO_2 hydrate, phase field theory and a model based on cellular automata. The two approaches are applied to simulations of hydrate growth from supersaturated aqueous solution of CO_2. The thermodynamic models for the solution properties are derived from experimental solubility data while the hydrate thermodynamics is based on adsorption theory with reference properties derived from molecular simulations. We show that the cellular automata approach has the benefit of being much more computationally efficient, and are still giving results which are consistent with results from the phase field theory.

Keywords Gas hydrates · CO_2 · Growth from solutions

1 Introduction

Gas hydrates are crystalline structures of water with cavities filled by small non-polar "guest" molecules, e.g. CO_2 or methane. The presence of these guest molecules can stabilise the ice-like structure at temperatures well above the melting point of pure ice. The kinetics of hydrate formation, as well as the macroscopic structure and surface properties of the formed hydrate, depends on the kinetics of mass transport, heat transport and the free energy changes related to the phase transition. Small free energy differences between hydrate and the original phase will typically lead to

T. Buanes · B. Kvamme (✉) · A. Svandal
Department of Physics and Technology, University of Bergen, Allégaten 55, 5007 Bergen, Norway
e-mail: bjorn.kvamme@ift.uib.no

T. Buanes
e-mail: Trygve.Buanes@ift.uib.no

A. Svandal
e-mail: Atle.Svandal@ift.uib.no

spherical-like hydrate particles and slurry-like hydrate floating in the aqueous phase. Large free energy differences will give rice to different types of branched crystals and typically less tendencies to agglomeration of individual crystals, which involves smaller risk for hydrate plugging in flowing systems.

In order to be able to model these phenomena we need theoretical approaches that are able to describe the kinetic progress in time and space as well as the corresponding crystal structures and surface properties. Using molecular dynamics simulations, microscopic properties of the growth processes can be investigated. But to learn about the structure at larger scales other tools, such as mean field theories, are required.

Mesoscopic modelling of hydrate growth has up to now mainly been done using phase field theory [1,2]. Although phase field theory primarily has been developed for modelling solidification of metallic melts, it also has potential for providing insight into the kinetics of hydrate growth.

Unfortunately, calculations based on phase field theory are generally very computationally intensive. This places strong restrictions on the system sizes and time spans which are feasible to simulate within this framework. As an attempt to overcome this challenge, we presented in [3] a simplified framework for simulating hydrate kinetics. This model will be referred to as cellular automata model.

In this work we investigate these two mean field approaches for this. The cellular automata model uses a Monte Carlo approach to evaluate the most probable growth paths. The phase field theory is based on the free energy functional related to the phase transition and involves the integration of a coupled set of differential equations in time and space. Both theories are outlined and calculated results for CO_2 hydrate growth from aqueous solution using two different geometries are compared.

2 Phase field theory

We employ a version of phase field theory which includes three fields: the phase, ϕ; molar CO_2 concentration, c; and microscopic orientation, θ. All fields are varying with time as well as position.

ϕ Appears as an order parameter, and can take values on the interval [0, 1]. Note that for historical reasons $\phi = 0$ corresponds to solid and $\phi = 1$ to liquid in the scope of phase field theory. Intermediate values of ϕ applies to the interface region between solid and liquid. In the case of CO_2 hydrate the thickness of this interface region has been measured in MD simulations to be 0.85 ± 0.07 nm.

The concentration field (c), is defined to be

$$c = \frac{x_{CO_2}}{x_{CO_2} + x_{H_2O}}, \tag{1}$$

where x_{CO_2} and x_{H_2O} is the number of CO_2 molecules and H_2O molecules, respectively, in the cell in question.

The orientation field θ is included to model the effect of differences in orientations of molecules in the solid phase. The inclusion of this field facilitates simulation of phenomena such as polycrystalline growth and anisotropies.

The basis of the model is the free energy functional,

$$F = \int d^3r \left(\frac{\varepsilon_\phi^2 T}{2} |\nabla \phi|^2 + \frac{\varepsilon_c^2 T}{2} |\nabla c|^2 + f \right), \tag{2}$$

where

$$\begin{aligned} f =& w(c) T g(\phi) + p(\phi) f_L(c, T) \\ &+ [1 - p(\phi)][f_S(c, T) + f_{\text{ori}}(|\nabla \theta|)]. \end{aligned} \tag{3}$$

Subject to conservation of the field c, the equations of motion are derived [4]:

$$\begin{aligned} \dot{\phi} &= M_\phi \frac{\delta F}{\delta \phi} + \zeta_\phi, \\ \dot{c} &= -\nabla \left(M_c \frac{\delta F}{\delta c} \right) + \zeta_c, \\ \dot{\theta} &= M_\theta \frac{\delta F}{\delta \theta} + \zeta_\theta. \end{aligned} \tag{4}$$

where $\delta F / \delta x$ indicates functional differentiation of the free energy functional (2) with respect to the fields. ε_θ, ε_c and $w(c)$ are related to the interface free energy, interface thickness and melting temperature [5], and can be obtained from experiments or molecular dynamics simulations.

The functions $g(\phi)$ and $p(\phi)$ are not completely fixed, but their form is constrained by the requirement of thermodynamical consistency [6]. f_L and f_S are the free energy densities of the aqueous solution and solid hydrate, respectively, and f_{ori} is an extra contribution added to take into account orientational differences in the solid phase. The terms ζ_i are Langevin noise terms added to model thermal fluctuations in the system.

The factors M_X are the mobilities of the fields. The phase field mobility, M_ϕ, dictates the rate of crystallisation. According to experiments [7–9] the crystallisation rate in highly under-cooled liquids is proportional to the transverse diffusion rate, D_{tr}, which is related to the viscosity, η, as $D_{\text{tr}} \propto \eta^{-0.74}$. Since the crystallisation rate in this model is proportional to M_ϕ, this implies $M_\phi \propto D_{\text{tr}}$. The concentration field mobility, M_c is directly proportional to the classical inter-diffusion coefficient for a binary mixture.

3 Monte carlo cellular automata

In [3] we proposed a model based on cellular automata combined with Monte Carlo for simulations of CO_2 hydrate growth. This approach is much simpler than phase field theory, and the primary goal is to have a more computationally efficient tool enabling us to study larger systems and longer time spans.

The basis of our model is Metropolis tests where the change in free energy as response to change of phase, or change in CO_2 concentration or temperature is

considered. As input we use the free energy parametrised with respect to phase, φ, ($\varphi = 1$ corresponds to solid hydrate, and $\varphi = 0$ corresponds to liquid water with dissolved CO_2),[1] CO_2 molar fraction, x_{CO_2}, and temperature T. In particular, each time step consist of three steps: solidification, CO_2 diffusion and temperature diffusion. The criteria for solidification is that a cell should have at least one solid neighbour, and that

$$r < e^{-\beta \Delta f(x_{CO_2},T)\left[1-\lambda(\Phi_n-6)\right]}, \tag{5}$$

where $0 \leq r \leq 1$ is a random number with a flat distribution, β is the characteristic energy for the solidification process, $\Delta f(x_{CO_2}, T)$ is the change in free energy if the cell with molar CO_2 concentration x_{CO_2} and temperature T changes its phase from liquid to solid, $\Phi_n = \sum_n \omega_n \varphi_n$ is a weighted sum over solid neighbours with weights $\omega_n = 2$ for nearest neighbours, $\omega_n = 1$ for next nearest neighbours and $\omega_n = 0$ otherwise. The Φ_n-term is included to take surface energy effects into account, and its strength is parametrised with λ. The diffusion of CO_2 is done using a Monte Carlo implementation of Fick's law. At each time step one of the nearest neighbours are drawn at random for each cell. The current

$$j_c = -D_c \Delta n_{CO_2}(1 + \delta_c), \tag{6}$$

where n_{CO_2} is proportional to the number density of CO_2 molecules and δ_c is a random number with a Gaussian distribution centred at 0, runs if

$$r < e^{-\beta \Delta f(j_c)}, \tag{7}$$

where $0 \leq r \leq 1$ is a random number with a flat distribution, β is the characteristic energy for the diffusion, D_c is the diffusion coefficient, and $\Delta f(j_c)$ is the change in free energy due to the current j_c. The temperature diffusion is done in the same way,[2] but with $\beta = 0$, such that the current

$$j_T = -D_T \Delta T(1 + \delta_T), \tag{8}$$

where D_T is the thermal diffusion coefficient and δ_T is a random number with a Gaussian distribution centred at 0, is exchanged. In our system the heat transport is much faster than the mass transport. Since Eq. 8 require $D_T < 0$ to be consistent, we must apparently choose D_c very small. But this would slow down the simulation considerably. To circumvent this we replace $D_T \rightarrow D_T/m$ and run the temperature diffusion m times.

[1] Note that this is the opposite convention as compared to phase field theory. Even though this may be a source of confusion, we choose to use this more conventional choice for the Cellular Automata since we are not restrained by history in this case.

[2] This is justified by starting with $\Delta Q/A\Delta t = -\kappa \Delta T/\Delta x$. The diffusion coefficient, D_T, is related to the thermal conductivity, κ, as $D_T = \kappa/\rho C$, where ρ is the density, and C is the heat capacity.

In addition, we also need to establish length and time scales since these are not inherently defined in this model. Since the phase can only take the values 0 (liquid) and 1 (solid), but nothing in between, we interpret the size of a cell to be of the same magnitude as the interface thickness between solid hydrate and an aqueous solution. The time scale is connected to the length scale by the diffusion rate.

4 Thermodynamics

The thermodynamical functions describing the system are common for both models. The free energy density is parametrised as a function of phase, CO_2 concentration, temperature and pressure. The dependence on pressure is not made explicit since we do our simulations at constant pressure.

4.1 Liquid thermodynamics

The free energy density of the liquid is obtained by taking the contributions from pure water and from CO_2 in infinite dilution, and adding to them a contribution to account for the mixing.

We do our simulations with a pressure of 150 bars and initial temperature in the liquid of $274K$. Under these conditions the aqueous solution is saturated at 3.3% CO_2 (obtained by extrapolating relevant data by Teng and Yamasaki [10]). Since we also want to do simulations with supersaturated solutions the liquid free energy density is extrapolated into the supersaturated region under the approximation that the activity coefficients follow the same concentration dependence as that fitted from saturated solutions.

4.2 Hydrate thermodynamics

The hydrate thermodynamics is based on a model by Kvamme and Tanaka [11] and van der Waals and Platteeuw [12]. The free energy density is given by

$$v_m f_S = x_{\mathrm{CO_2}} g_{\mathrm{CO_2}} + (1 - x_{\mathrm{CO_2}}) g_w, \tag{9}$$

where v_m is the molar volume of the hydrate, and g_w and $g_{\mathrm{CO_2}}$ are partial molar free energies for water and CO_2 in the hydrate, respectively, given by

$$g_w = g_w^0 + \mathrm{RT}\nu \log(1 - \theta), \tag{10}$$

$$g_{\mathrm{CO_2}} = \Delta g^{\mathrm{inc}} + \mathrm{RT} \log\left(\frac{\theta}{1 - \theta}\right). \tag{11}$$

Here g_w^0 is the free energy density of water in empty hydrate, Δg^{inc} is the free energy of inclusion of gas molecules in the hydrate, $\theta = x_{\mathrm{CO_2}}/\nu(1 - x_{\mathrm{CO_2}})$ is the filling fraction of the cavities accessible to the CO_2 molecules, and ν is the number of accessible cavities per water molecule.

5 Simulation setup

We do simulations on a two dimensional system of size 128×128 nm. Since we are presently not able to handle nucleation we start with some hydrate present. The rest of the simulation window is filled with an aqueous solution with 3.3% CO_2. We use periodic boundary conditions on the simulation window.

We consider two different geometries:

(1) A small nucleus in the centre of the simulation window. Since the system is isotropic, this is expected to grow to a circular piece of hydrate.
(2) A thin strip of hydrate passing vertically through the centre of the simulation window. This system aims to simulate the growth of a hydrate film.

A more interesting version of the latter system would be the growth of a hydrate film on the interface between liquid CO_2 and liquid water with dissolved CO_2. We can do simulations on this setup using phase field theory, but at present we are not able to do this with the cellular automaton model. The phase field simulations shows, however, that almost all growth takes place on the water side, whereas the CO_2 side is almost static. Therefore, the setup with aqueous solution on both sides of the film gives relevant information also for the more interesting system with liquid CO_2 on the side.

6 Results

In the first setup both models produce compact hydrate particles, but the cellular automaton approach gives rise to a slightly less regular particle than the perfect circular particle produced by the phase field theory, see Fig. 1. As shown in [3] the morphology of the hydrate particle produced by the cellular automaton approach is strongly dependent on the driving forces, large driving forces giving rice to branched structures. By replacing $\varepsilon_\phi \rightarrow \varepsilon_\phi[1 + s_0 \cos(n\vartheta - 2\pi\theta)]/2$ in Eq. 2, where $\vartheta = \arctan[(\nabla\phi)_y/(\nabla\phi)_x]$ and n is an integer describing the symmetry of the system, branching can also be seen within the scope of phase field theory [13]. The parameter s_0 determines the strength of the anisotropic effect introduced by this modification.

Monitoring the growth rate, measured in terms of fraction of the system converted into hydrate, we find that the models are in good agreement at short times as shown

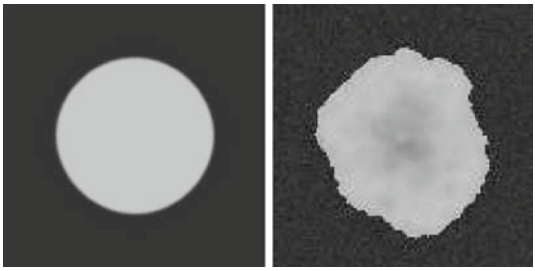

Fig. 1 Hydrate particle after 5.6 μs. The system is 128×128 nm. *Left* Phase field theory simulation. *Right* Cellular automaton simulation

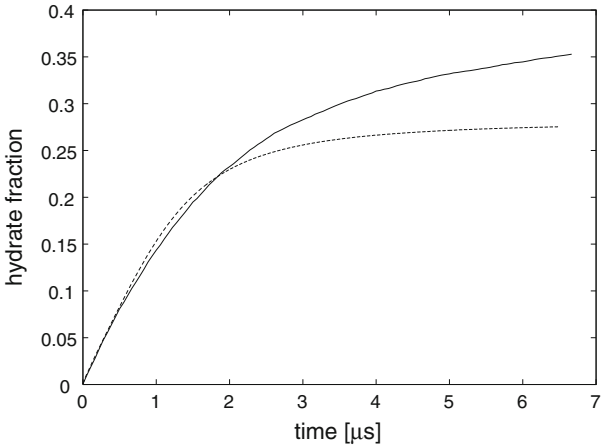

Fig. 2 Fraction of total system converted into hydrate as a function of time [system (1)]. *Dashed line* Phase field theory simulation. *Solid line* Cellular automaton simulation

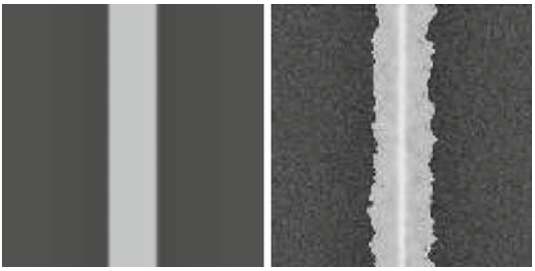

Fig. 3 Hydrate film after 1.7 μs. The system is $128 \times 128\,nm$. *Left* Phase field theory simulation. *Right* Cellular automaton simulation

in Fig. 2. However, the phase field simulation approaches a lower asymptotic value than the cellular automaton simulation. The reason for this is that the hydrate grown in the cellular automaton simulation has a little smaller CO_2 concentration than that of the phase field simulation. This difference becomes increasingly important as the CO_2 from the aqueous solution is consumed by the growing hydrate particle.

The hydrate film simulation shows the same general appearance as the hydrate ball; in both models the film thickness grows with approximately uniform thickness, see Fig. 3. Again, the cellular automaton model produces a slightly less regular growth than the phase field model. Comparing the growth rate we find that also using this geometry the rates are similar at small times. At larger times the same deficiency as for the hydrate ball geometry appears, and the growth rates starts to differ.

Considering the computational efficiency of the two approaches, we find that the cellular automaton simulations is nearly a factor of 75 faster than the phase field simulation. This is mainly due to the fact that in the cellular automata we can use larger

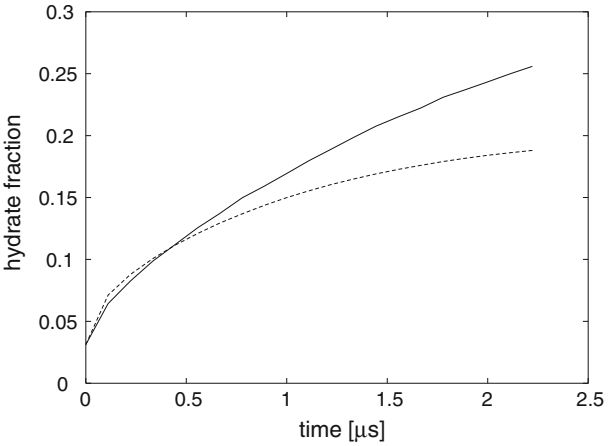

Fig. 4 Fraction of total system converted into hydrate as a function of time (system (2)). *Dashed line* Phase field theory simulation. *Solid line* Cellular automaton simulation

grid spacing and longer time steps. In simulations where temperature effects can be neglected, the speed-up of the cellular automaton approach will be even larger.

7 Conclusion

We have considered simulations of CO_2 hydrate growth using a phase field theory and a model based on cellular automata. The cellular automaton approach is certainly less rigorous than the phase field theory. The main problem is that there are several parameters which are hard to find correct values for from experiments or from more fundamental considerations. In particular, the characteristic energies used in the Metropolis tests, and the noise terms added to the diffusion currents are hard to quantify. But the simplicity of the model is also its strength; we have seen that using the cellular automaton approach simulations are done much more efficiently and thus allows for larger systems and longer time spans.

We have demonstrated that for two different geometries the evolutions of the systems are similar using both models, but there are some discrepancies at late times, probably due to finite size effects.

Presently the phase field theory is by far the most mature of the two approaches, but the computational efficiency of the cellular automata makes this model an interesting supplement to the more rigorous calculations of the phase field theory. Thus doing simulations on small systems the phase field theory can be used to calibrate the free parameters of the cellular automata model. Then the latter model can be used to perform simulations of larger systems, which are not feasable to do using phase field theory due to the computational demands.

Acknowledgements This work has been supported financially by The Research Council of Norway and Hydro. We would also like to thank Laszlo Gránásy whose contribution in the phase field theory simulations has been invaluable.

References

1. B. Kvamme, A. Graue, E. Aspenes, T. Kuznetsova, L. Gránásy, G. Tóth, T. Pusztai, G. Tegze, Kinetics of solid hydrate formation by carbon dioxide: phase field theory of hydrate nucleation and magnetic resonance imaging. Phys. Chem. Chem. Phys. **6**(9), 2327–2335 (2003)
2. B. Kvamme, L. Gránásy, T. Kuznetsova, A. Svandal, T. Buanes, Towards a kinetic model for hydrate sealing of CO_2 in reservoirs, in *7th International Conference on Greenhouse Gas Control Technologies* (2004)
3. T. Buanes, B. Kvamme, A. Svandal, Computer simulation of CO_2 hydrate growth. J. Crys. Growth **287**, 491–494 (2006)
4. L. Gránásy, T. Pusztai, J. Warren, Modelling polycrystalline solidification using phase field theory. J. Phys. Condens. Matter **16**(41), R1205–R1235 (2004)
5. L. Gránásy, T. Pusztai, G. Tóth, Z. Jurek, M. Conti, B. Kvamme, Phase field theory of crystal nucleation in hard sphere liquid. J. Chem. Phys. **119**(19), 10376–10382 (2003)
6. S.L. Wang, R.F. Sekera, A.A. Wheeler, B.T. Murray, S.R. Coriell, R.J. Braun, G.B. McFadden, Thermodynamically consistent phase-field models for solidification. Physica D **69**, 189–200 (1993)
7. A. Masuhr, T.A. Waniuk, R. Busch, W.L. Johnson, Time scales for viscous flow, atomic transport, and crystallization in the liquid and supercooled liquid states of $zr_{41.2}ti_{13.8}cu_{12.5}ni_{10.0}be_{22.5}$. Phys. Rev. Lett. **82**(2290–2293) (1999)
8. K.L. Ngai, J.H. Magill, D.J. Plazek, Flow, diffusion and crystallization of supercooled liquids: revisited. J. Chem. Phys. **112**, 1887–1892 (2000)
9. S.F. Swallen, P.A. Bonvallet, R.J. McMahon, J.D. Ediger, Self-diffusion of tris-naphthylbenzene near the glass transition temperature. Phys. Rev. Lett. **90**, 015901 (2003)
10. H. Teng, A. Yamasaki, Solubility of liquid CO_2 in synthetic sea water at temperatures from 278K to 293K and pressures from 6.44MPa to 29.49MPa, and denisities of the corresponding solutions. J. Chem. Eng. Data **43**(1), 2–5 (1998)
11. B. Kvamme, H. Tanaka, Thermodynamic stability of hydrates for ethane, ethylene and carbon dioxide. J. Phys. Chem. **99**, 7114–7119 (1995)
12. J.H. van der Waals, J.C. Platteeuw, Clathrate solutions. Adv. Chem. Phys. **2**, 1–57 (1959)
13. A. Svandal, B. Kvamme, L. Gránásy, T. Pusztai, The influence of diffusion on hydrate growth. J. Phase Equlib. Diffus. **26**(5), 534–538 (2005)